

Solar radio emission below the ionospheric cutoff: theory and phenomenology

Stuart D. Bale

University of California, Berkeley

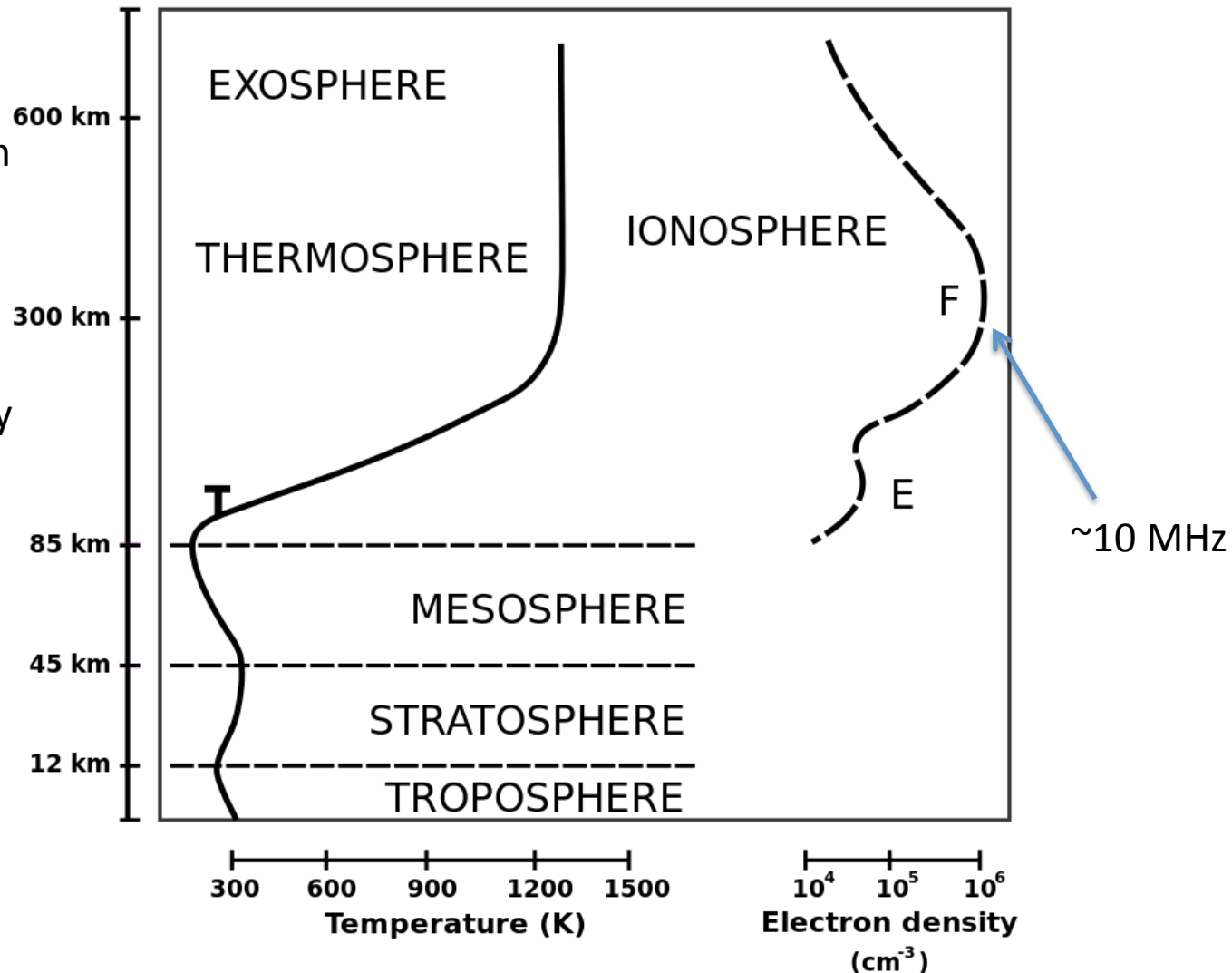
outline

- 1) Terrestrial ionosphere
- 2) reflection of radio waves and frequency range
- 3) solar wind density profile and corresponding frequency range
- 4) emission mechanisms
- 5) phenomenology
 - a) type II and type III bursts, terrestrial electron foreshock, Jupiter
 - b) fundamental and harmonic emission
 - c) no polarization
 - d) beam pattern
- 6) plasma emission theory
 - a) electron beams
 - I) origin, advection, observations
 - b) Langmuir waves growth, beam saturation, Sturrock's dilemma
 - c) mode conversion
 - I) linear mode conversion
 - II) three wave coupling - random phase approximation

The terrestrial ionosphere

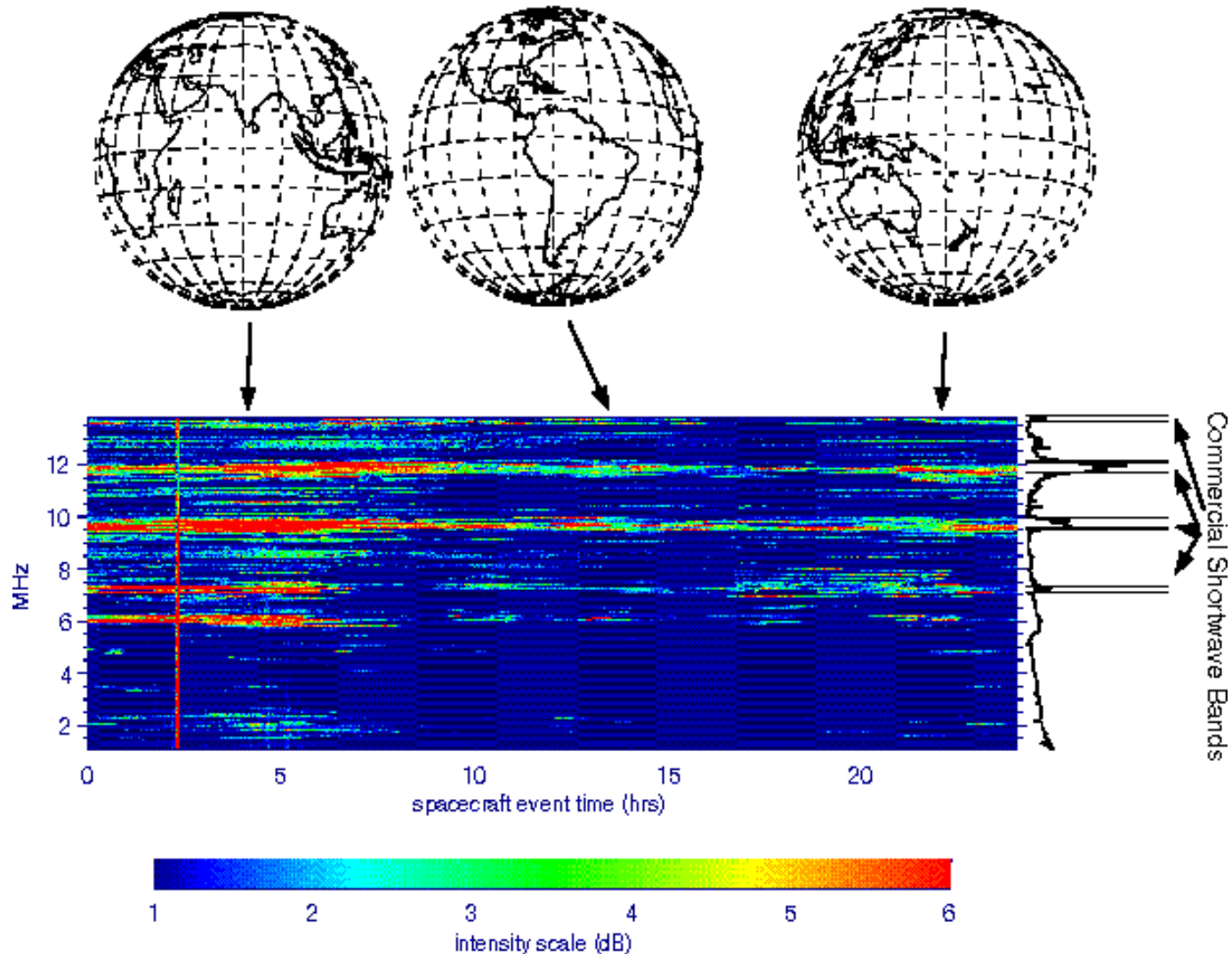
- UV ionization
- Recombination
- F-layer 200-1000km
- Diurnal variations
- Seasonal variations

- F-layer peak density is $\sim 10^6 \text{ cm}^{-3}$
- Corresponding plasma frequency $\sim 10 \text{ MHz}$
- We need to get above $\sim 500 \text{ km}$ to get to lower frequencies



Man-made interference

WIND/WAVES November 17, 1994



e/m waves near f_{pe} in cold plasma

Summary of electromagnetic electron waves

conditions	dispersion relation	name
$\vec{B}_0 = 0$	$\omega^2 = \omega_p^2 + k^2 c^2$	light wave
$\vec{k} \perp \vec{B}_0, \vec{E}_1 \parallel \vec{B}_0$	$\frac{c^2 k^2}{\omega^2} = 1 - \frac{\omega_p^2}{\omega^2}$	O wave
$\vec{k} \perp \vec{B}_0, \vec{E}_1 \perp \vec{B}_0$	$\frac{c^2 k^2}{\omega^2} = 1 - \frac{\omega_p^2}{\omega^2} \frac{\omega^2 - \omega_p^2}{\omega^2 - \omega_h^2}$	X wave
$\vec{k} \parallel \vec{B}_0$ (right circ. pol.)	$\frac{c^2 k^2}{\omega^2} = 1 - \frac{\omega_p^2/\omega^2}{1 - (\omega_c/\omega)}$	R wave (whistler mode)
$\vec{k} \parallel \vec{B}_0$ (left circ. pol.)	$\frac{c^2 k^2}{\omega^2} = 1 - \frac{\omega_p^2/\omega^2}{1 + (\omega_c/\omega)}$	L wave

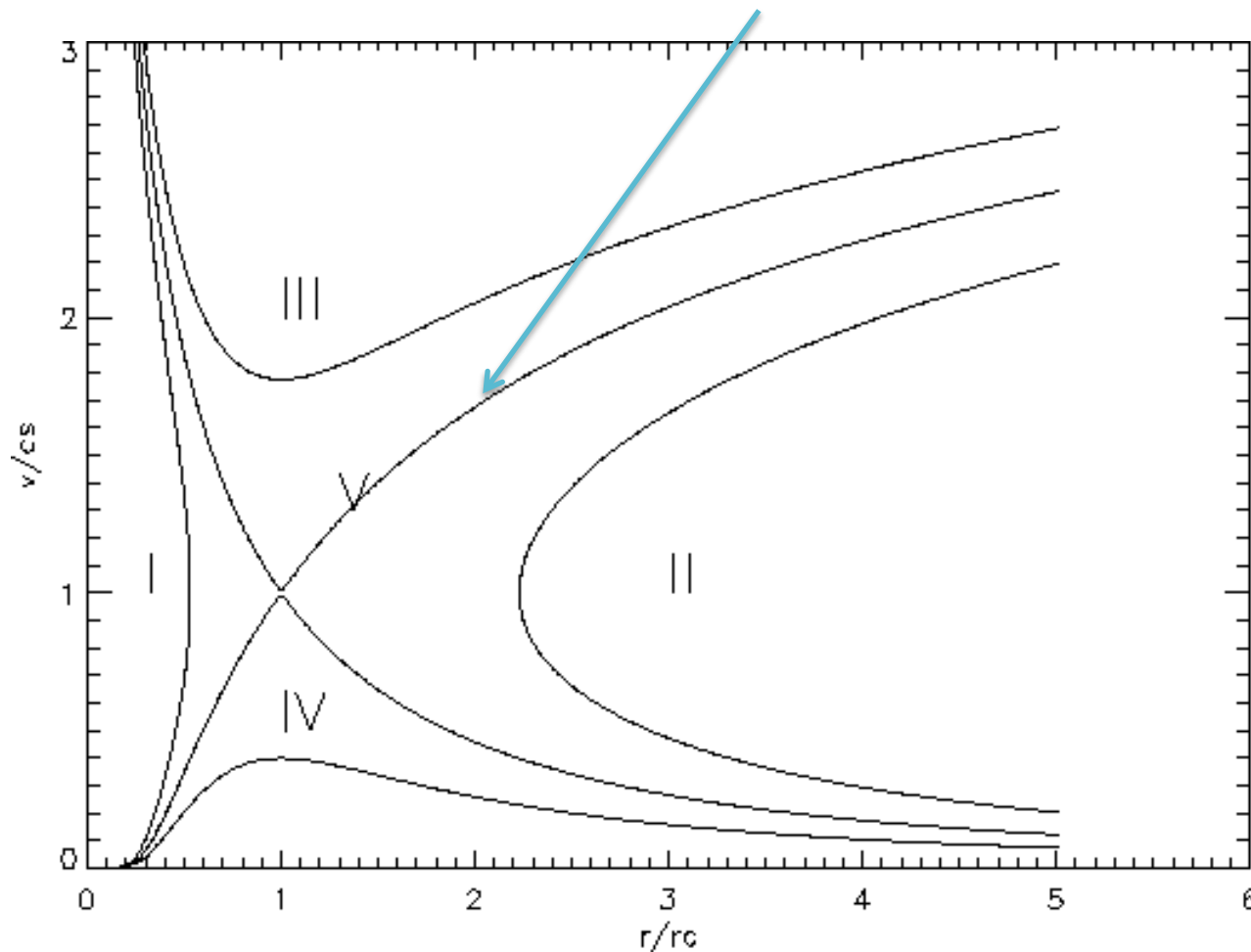
We also need Langmuir waves and ion sound waves

$$\omega^2 = \omega_{pe}^2 + 3/2 k^2 v_{th}^2 \quad \text{and} \quad \omega = k c_s$$

Source regions: Parker's solar wind model

- Hydrostatic solution (similar to Bondi accretion)
- Predicts a supersonic atmosphere 'wind'
- Similar to 'de Laval nozzle' or a jet engine
- Requires energy input at the base. kT_{ph} is not nearly enough! Requires nonthermal energy
- 'Alfven point' in magnetized plasma determines extent of corona - corotation

A 'solar wind' is accelerated from the corona



Solar wind acceleration profiles

'Fast' and 'slow' profiles

Fast wind is relatively uniform

Slow solar wind is blobby

Minor ions show enhanced acceleration – field-aligned flow

Flux conservation gives us a density profile...

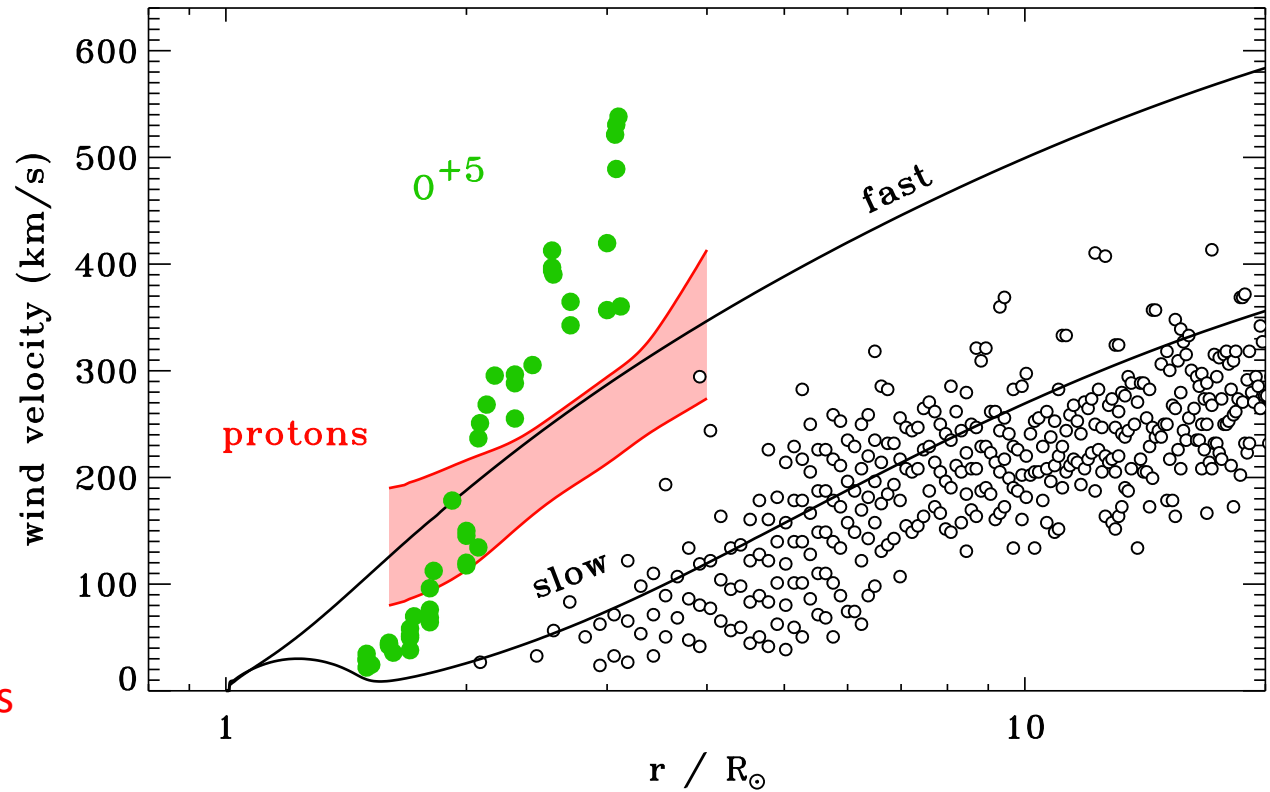
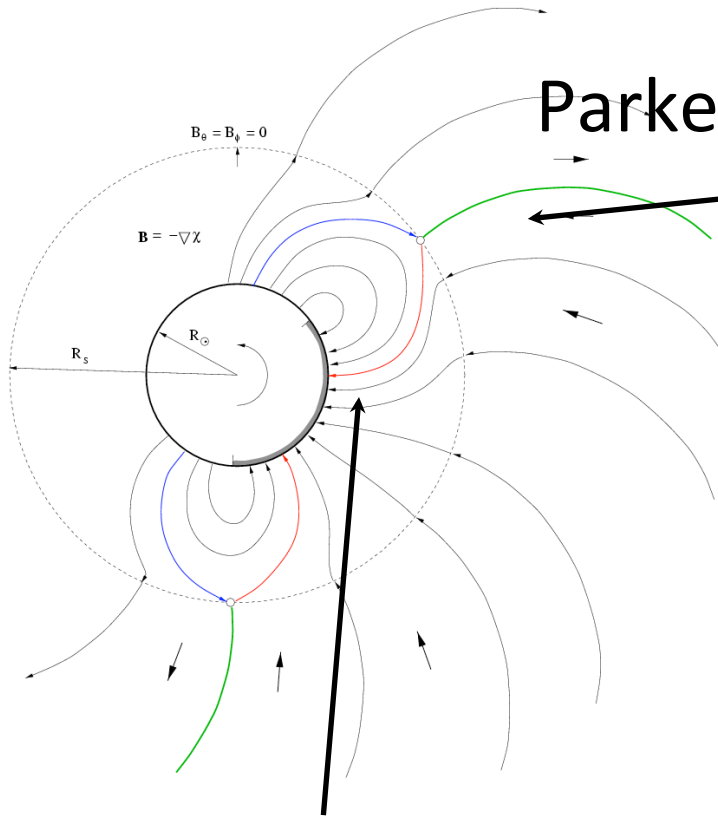


Figure 8: Radial dependence of solar wind outflow speeds. UVCS Doppler dimming determinations for protons (red; Kohl *et al.*, 2006) and O⁺⁵ ions (green; Cranmer *et al.*, 2008) are shown for polar coronal holes, and are compared with theoretical models of the polar and equatorial solar wind at solar minimum (black curves; Cranmer *et al.*, 2007) and the speeds of “blobs” measured by LASCO above equatorial streamers (open circles; Sheeley Jr *et al.*, 1997).

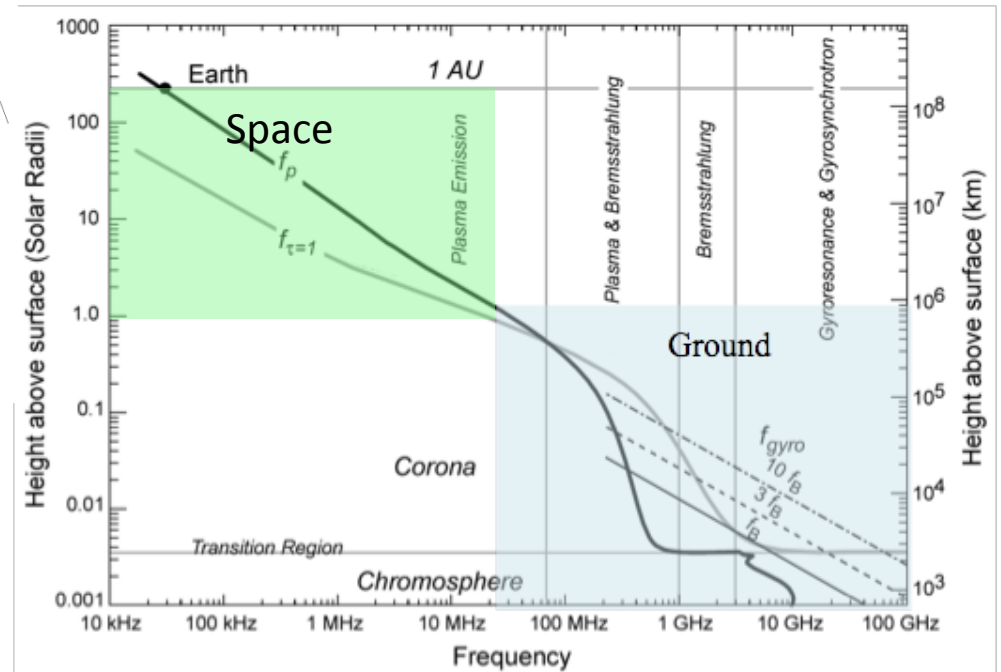
(Cranmer, 2009)

'Interplanetary radio bursts' - the inner heliosphere



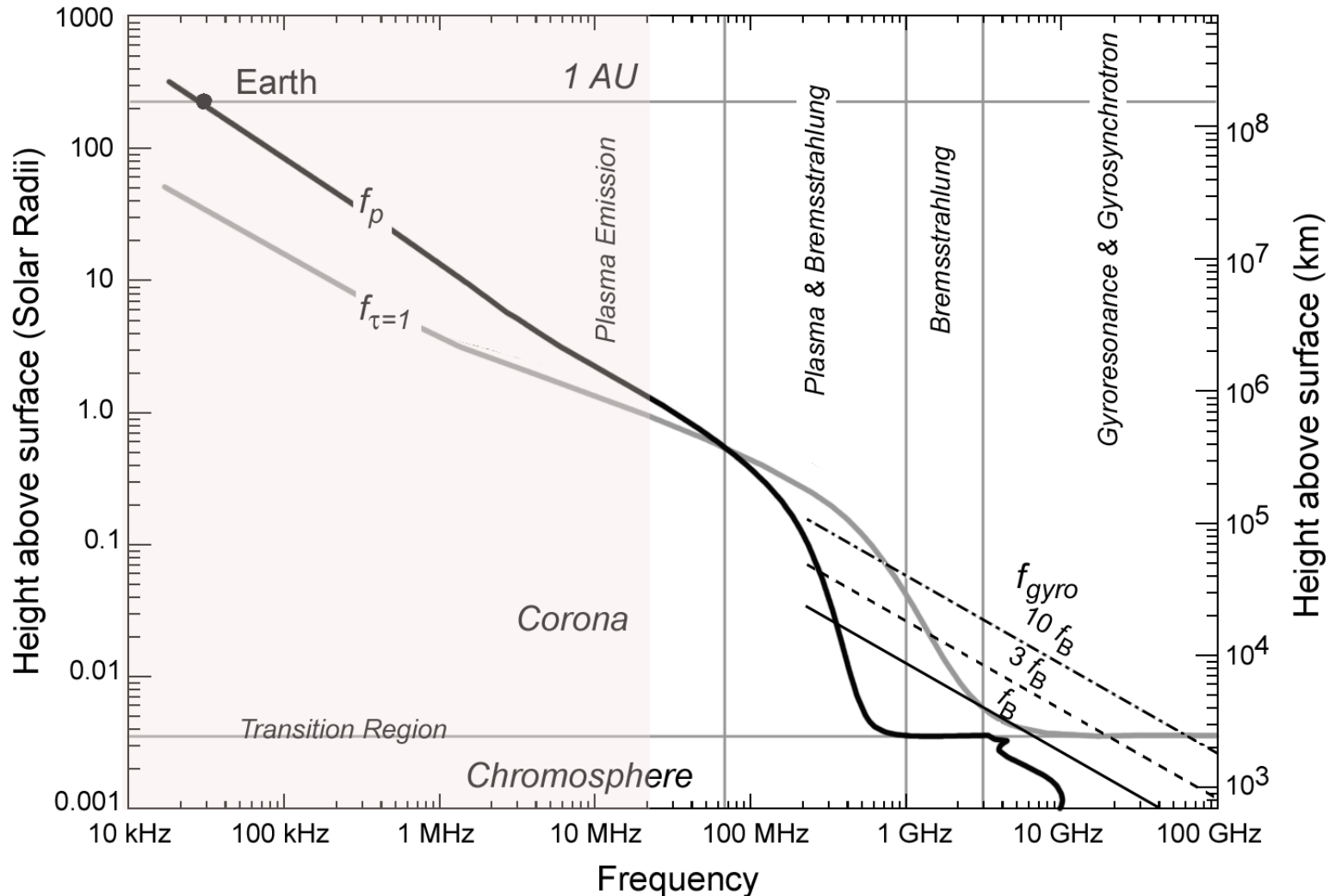
Parker spiral field,
spherical expansion

More complicated,
dynamic field; wind
acceleration



Emission mechanisms vs altitude:

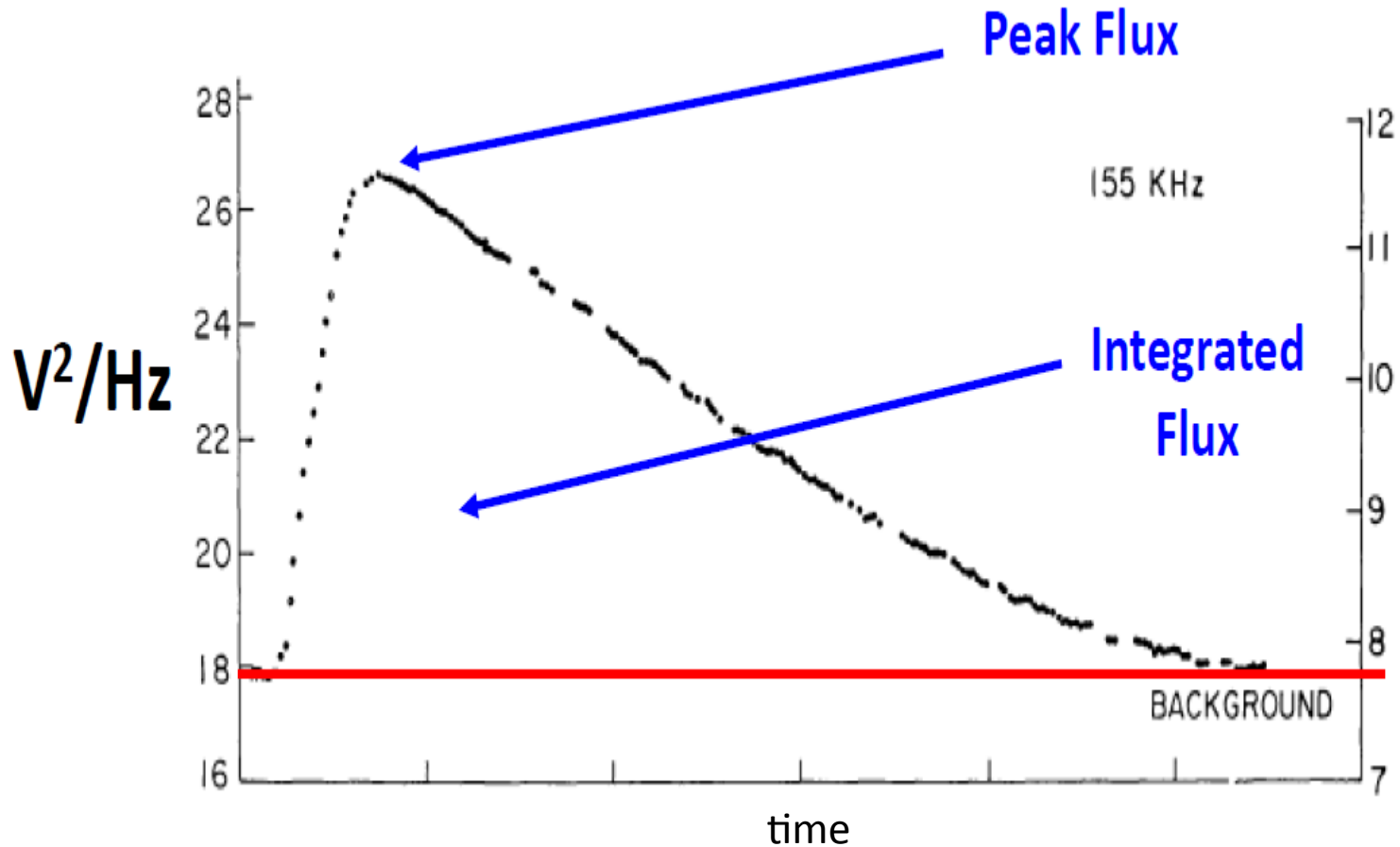
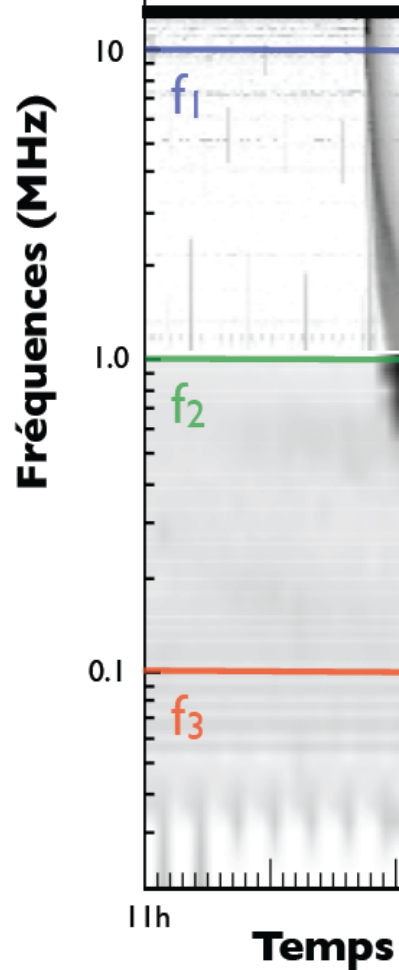
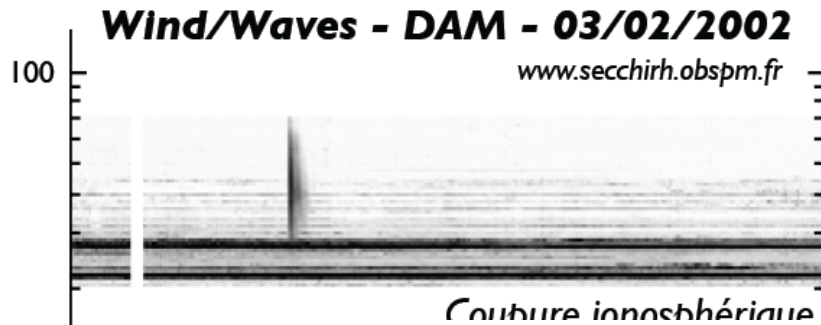
plasma emission dominates



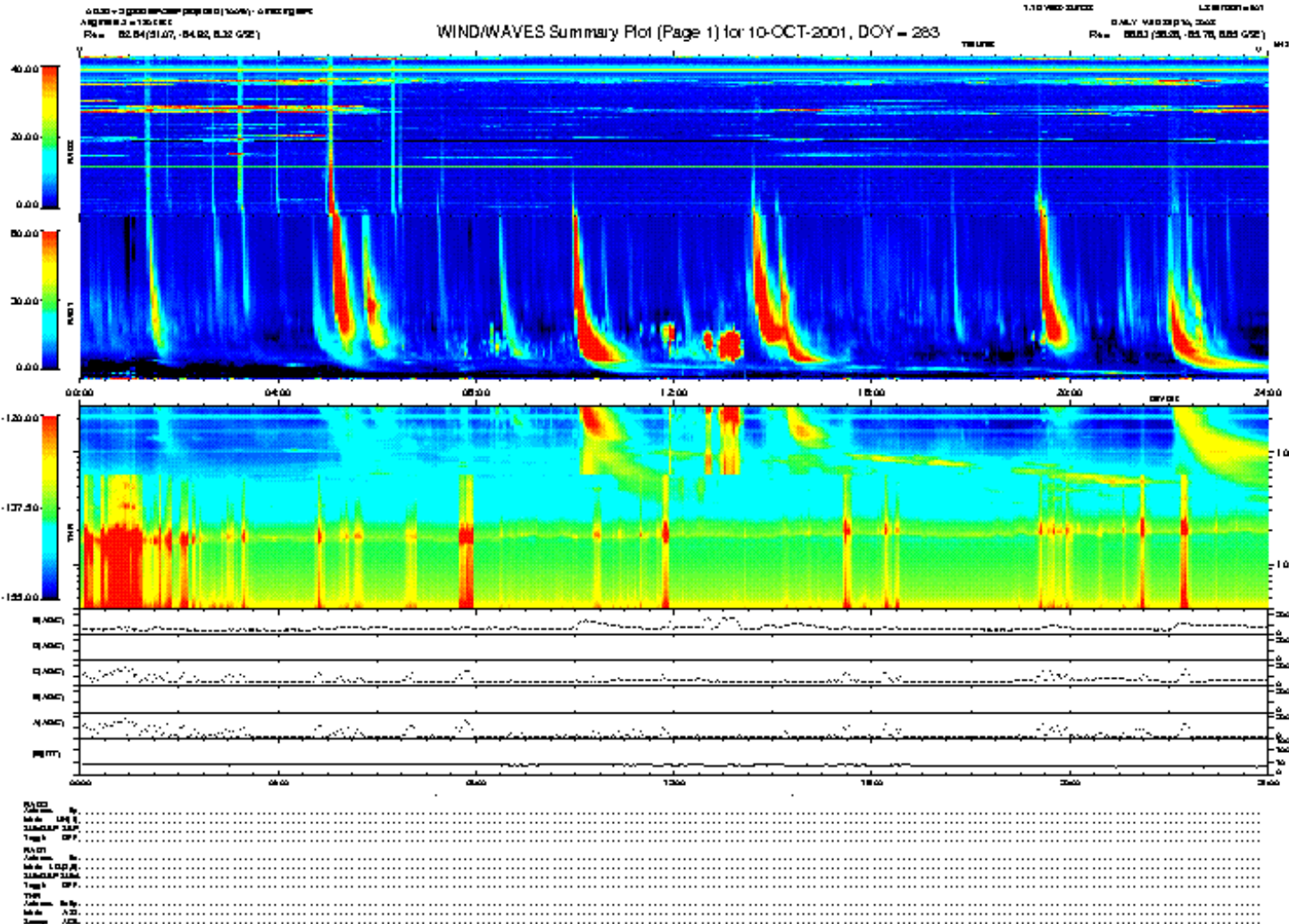
Primarily 'type II' and 'type III' interplanetary radio bursts

First observations by Wild, 1950

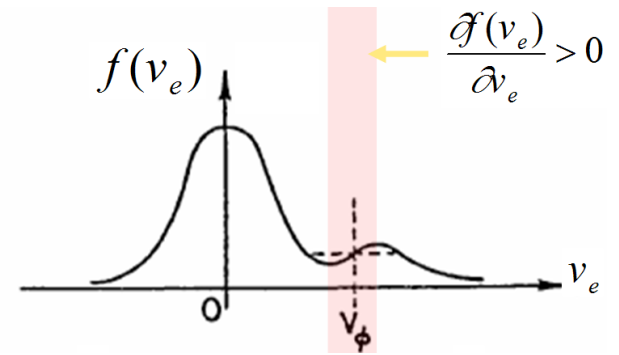
- Rapid (sec \rightarrow hrs) & very intense ($\rightarrow 10^{-14} \text{ W.m}^{-2}.\text{Hz}^{-1}$) radio emissions



IP Radio Bursts - Phenomenology



Type III radio emission scenario

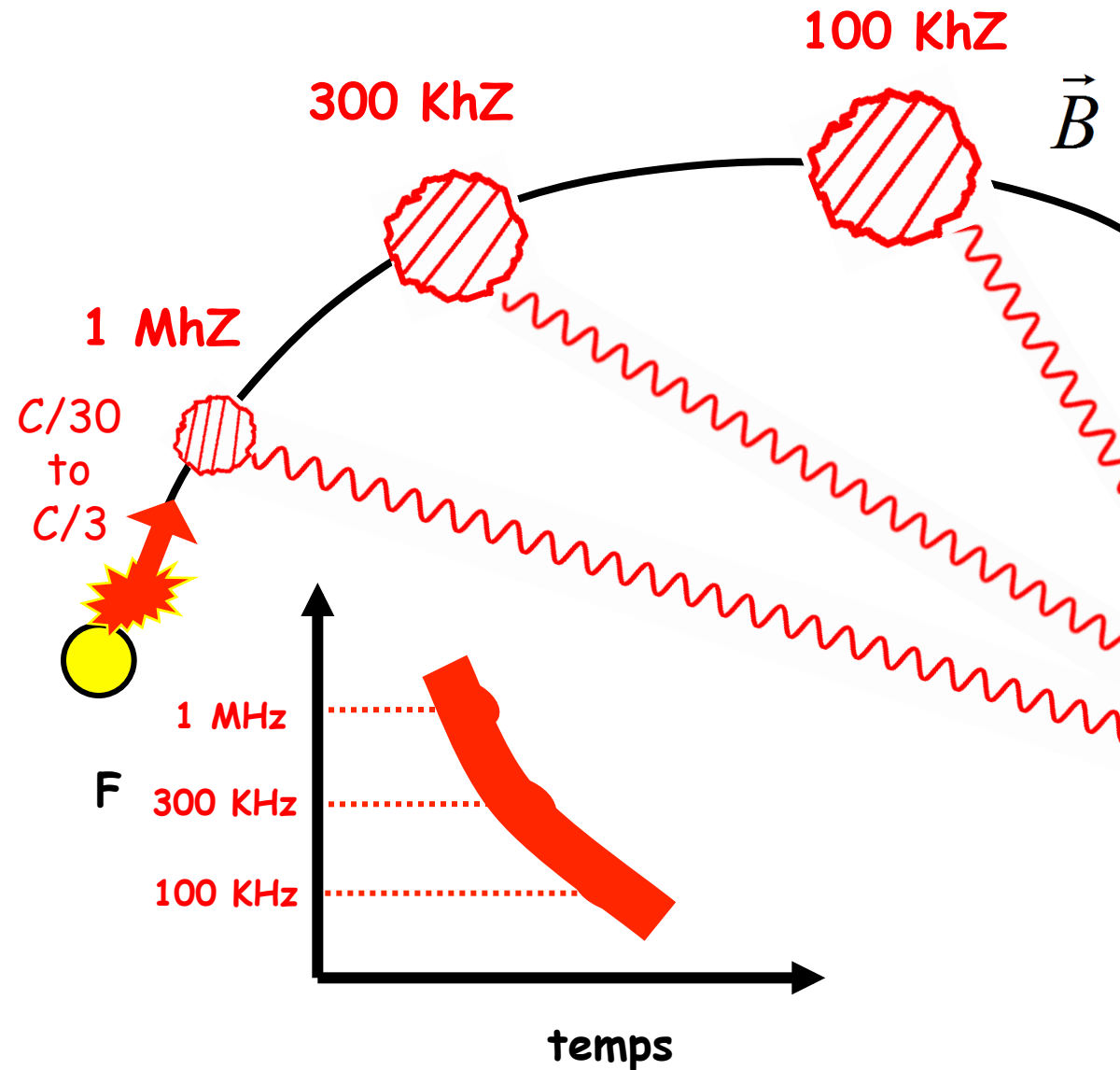


**Mode conversion
from Langmuir (e/s)
to e/m**

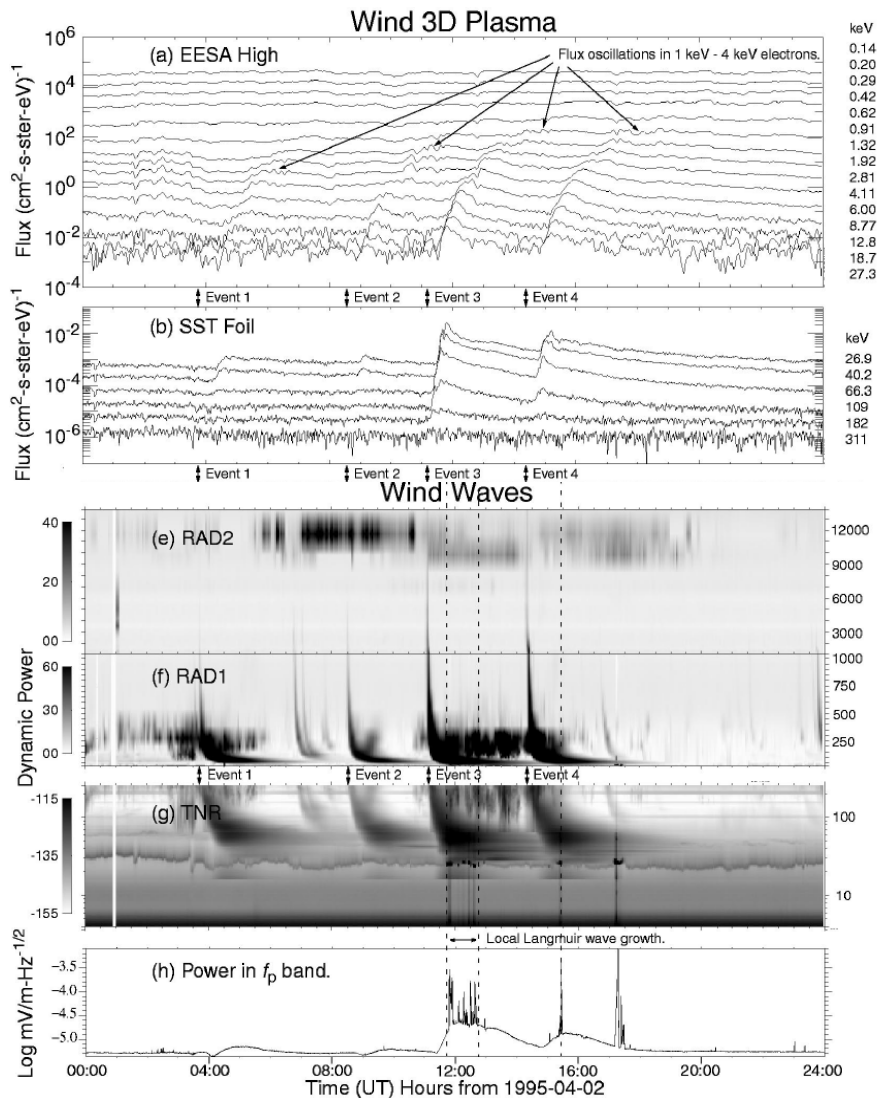
$$F_p \text{ (kHz)} \propto \sqrt{N_e \text{ (cm}^{-3}\text{)}}$$

$$N_e \propto 1/R^2 \text{ (au)}$$

$$\rightarrow F_p \propto \frac{1}{R}$$

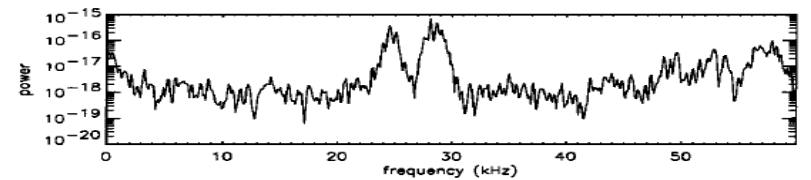
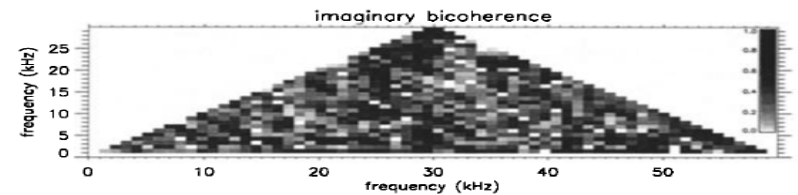
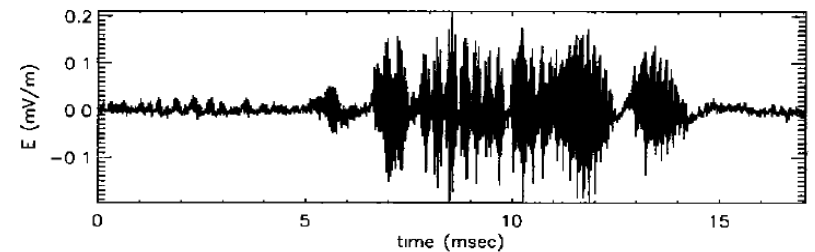


In-situ Type III measurements



The basic scenario is right:

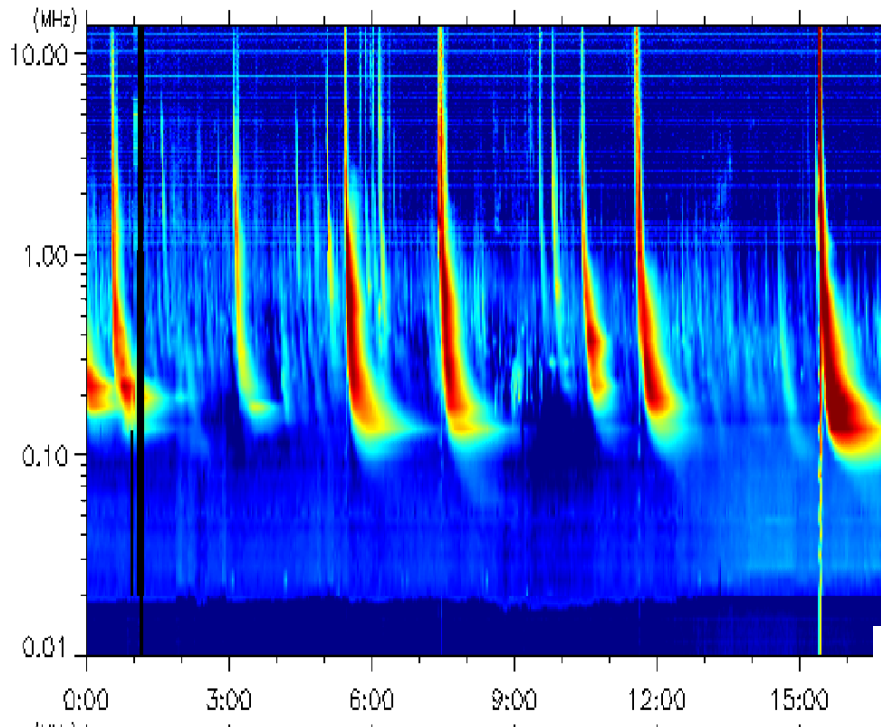
- Electron injection associated with flare
- Advection creates 'beam'
- Langmuir wave growth
- Mode conversion to *unpolarized e/m*



Bale et al., 1996, Evidence of three wave-coupling in the upstream solar wind

Adapted from [Ergun et al., 1998]

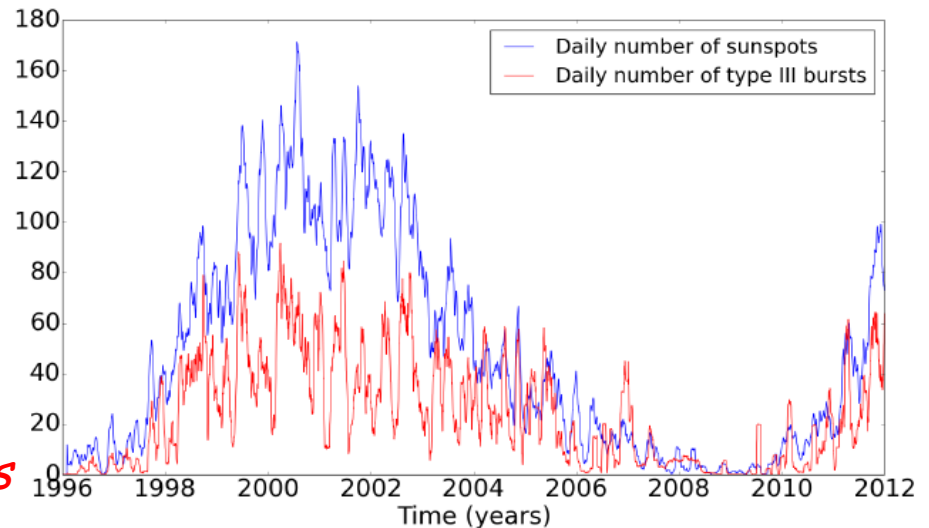
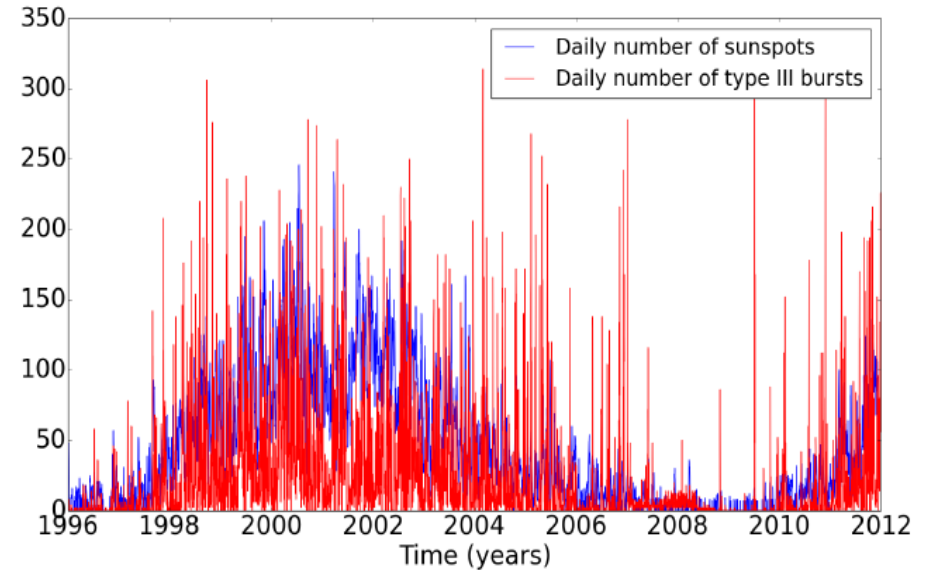
Occurrence of Type III radio bursts over a Solar Cycle



Automatic detection techniques

- *Lobzin et al. 2010*
- *Bonnin, 2008*

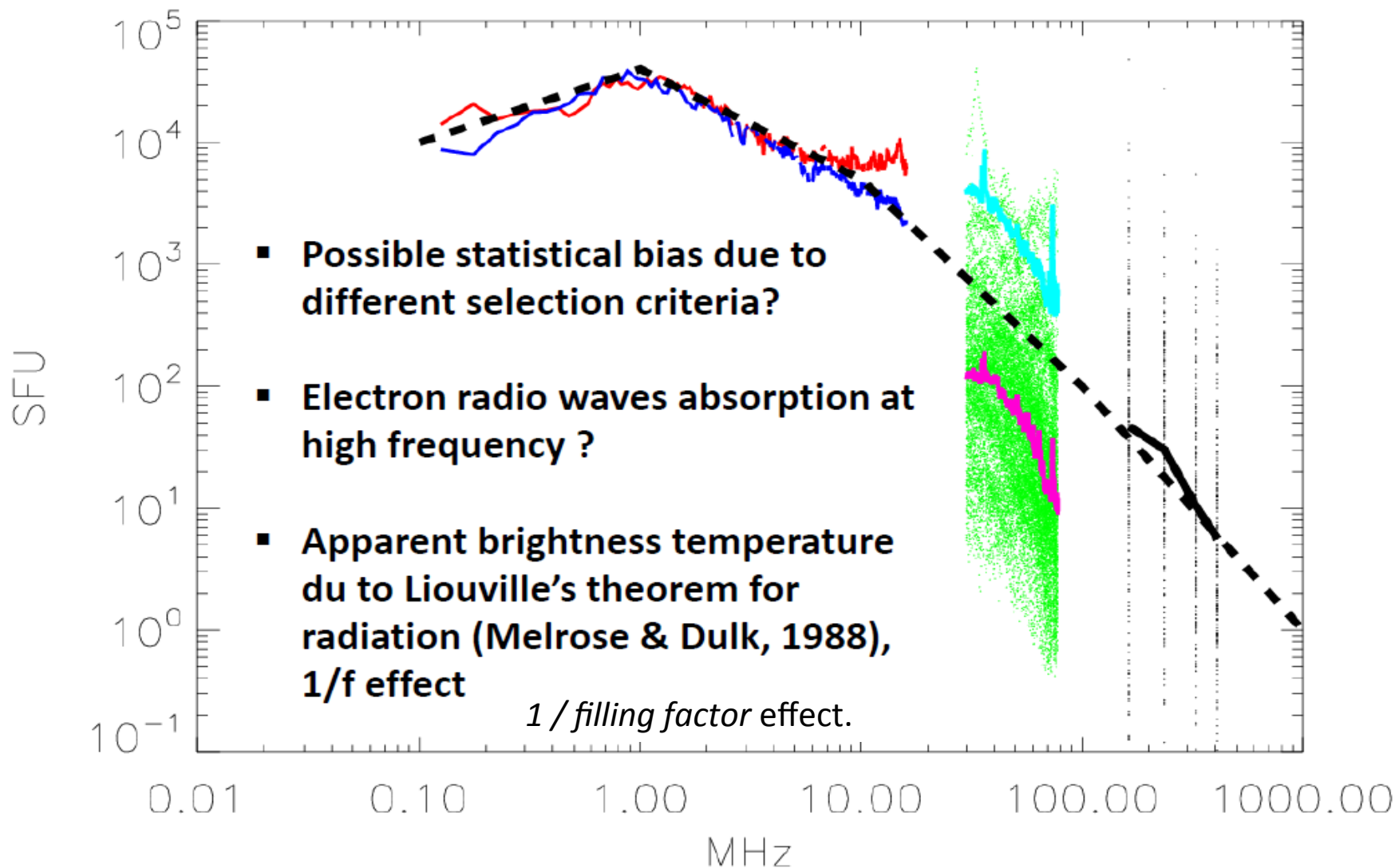
cor > 0.9 for smoothing window > 90 days
A. Navrer-Agasson & D. Sperone



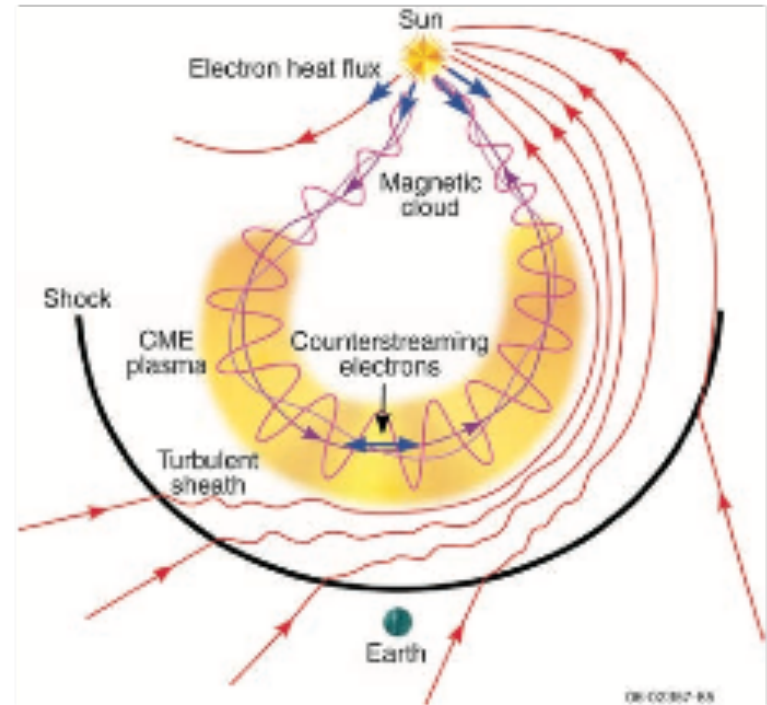
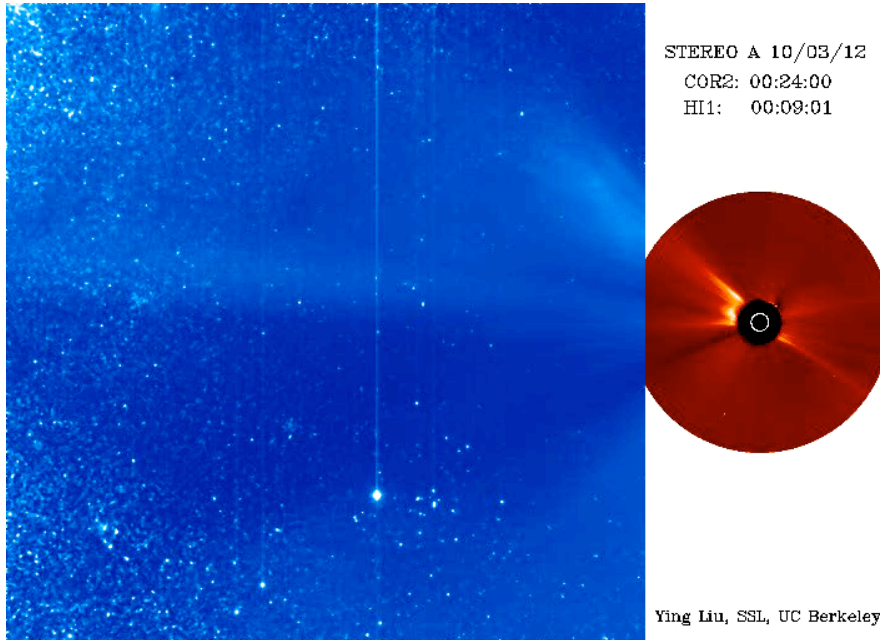
(b) Smoothed over 31 days

Peak intensity at around ~1 MHz

STEREO + DAM + NRH

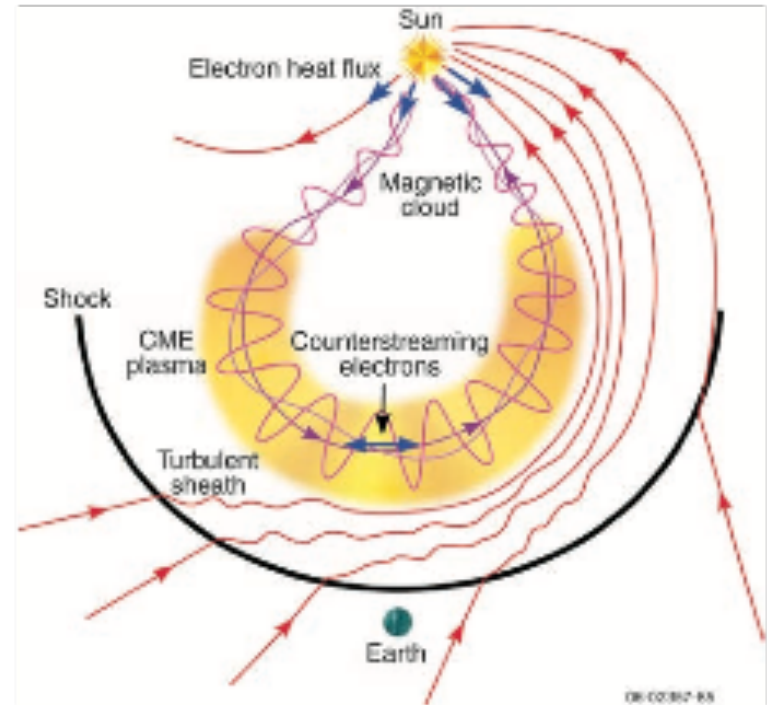
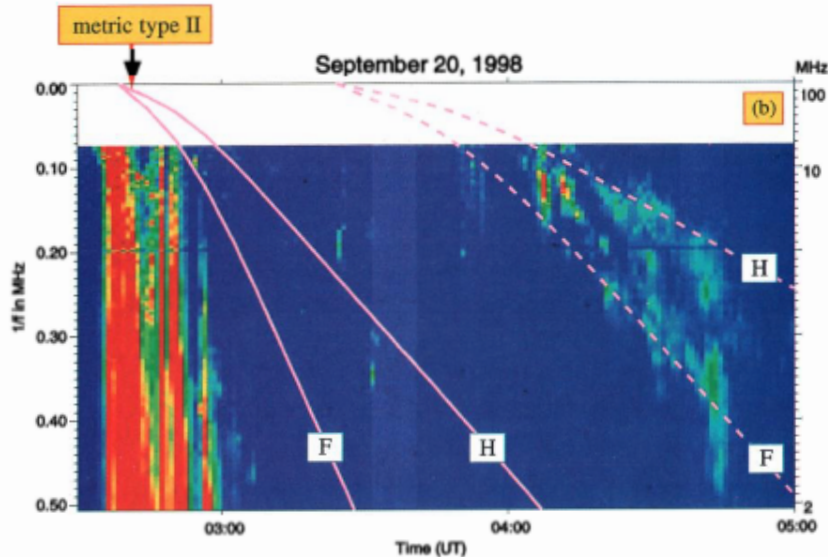
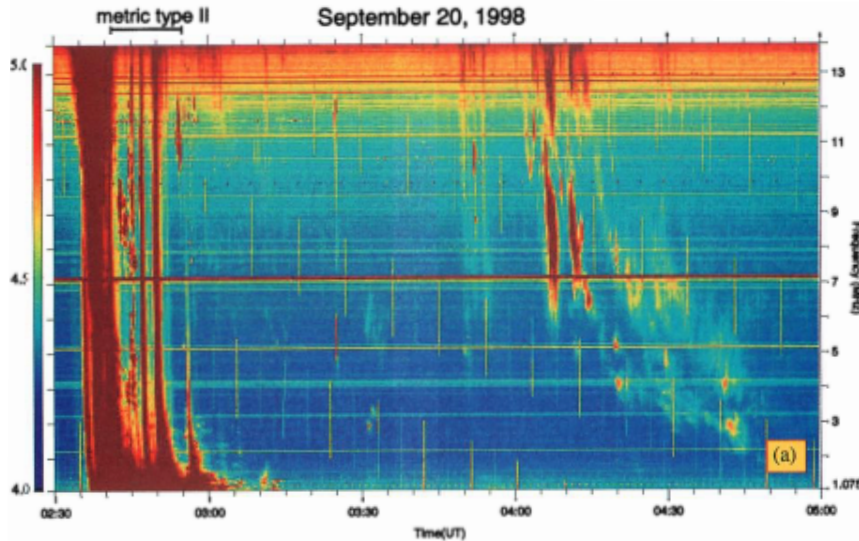


IP Radio Bursts - 'Type II' Radio Bursts



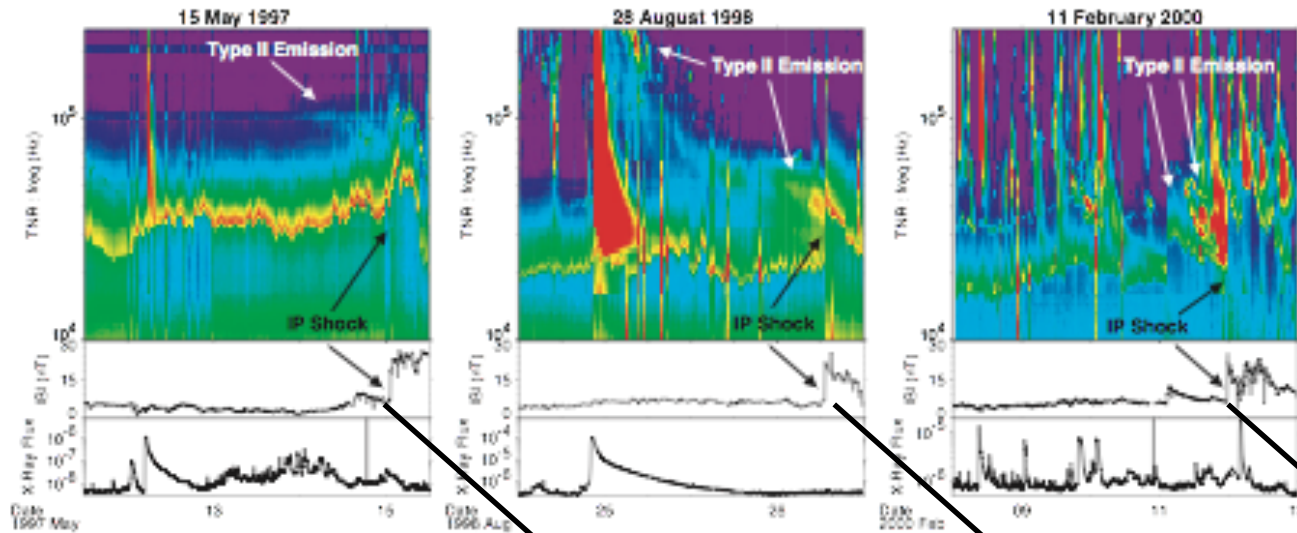
- Associated with 'fast' coronal mass ejections
- Electrons energized to 1-10 keV by CME-driven shock
- Radiation by plasma emission (f_{pe} and/or $2f_{pe}$)

IP Radio Bursts - 'Type II' Radio Bursts

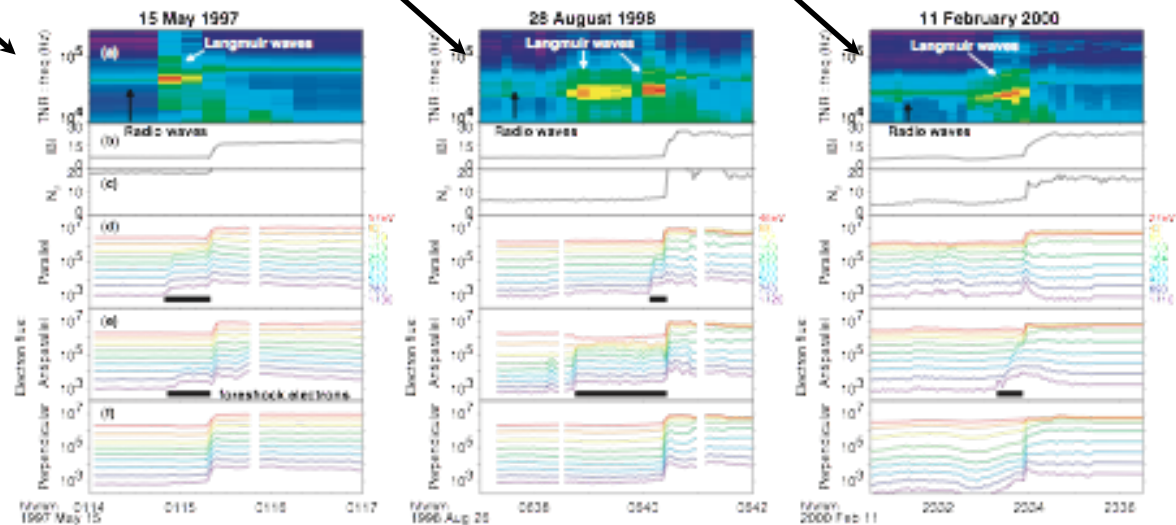
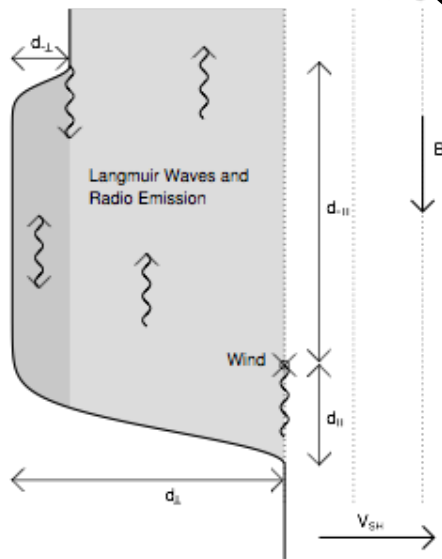


- Radiation by plasma emission (f_{pe} and/or $2f_{pe}$)
- Frequency drift rate is a measure of shock speed
- Fine structure implies multiple source regions

Physics - Shock Structure and Dynamics

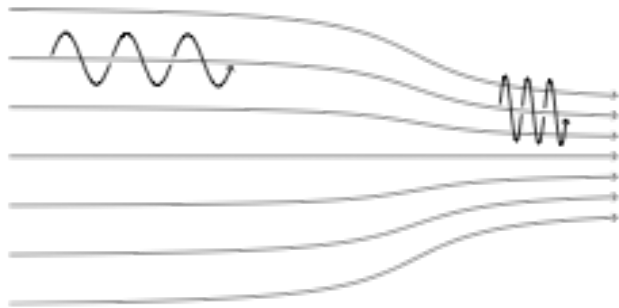


Real-life type II shocks give information about this structure

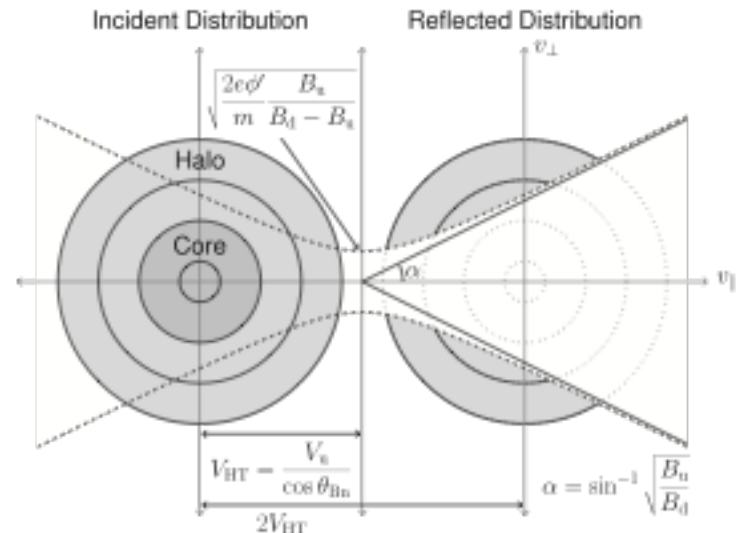


Physics - Electron Energization

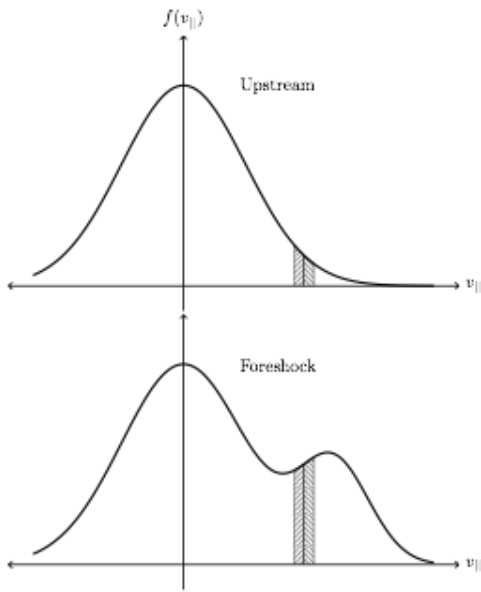
fast-Fermi acceleration



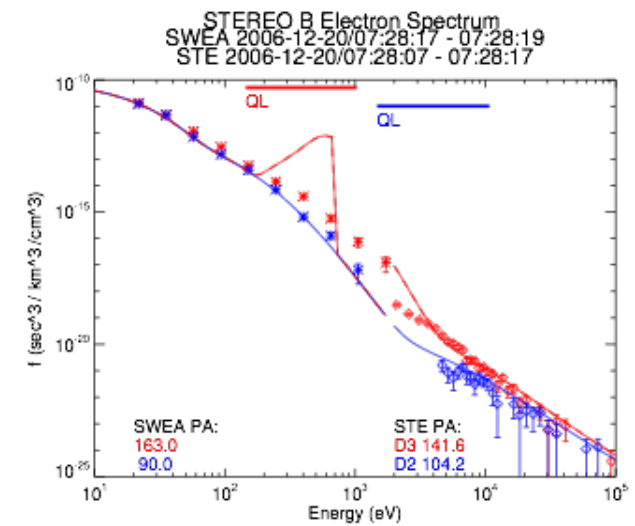
+



+



=



(Pulupa et al.)

e/m waves near f_{pe} in cold plasma

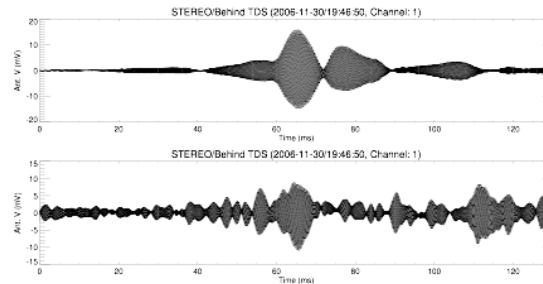
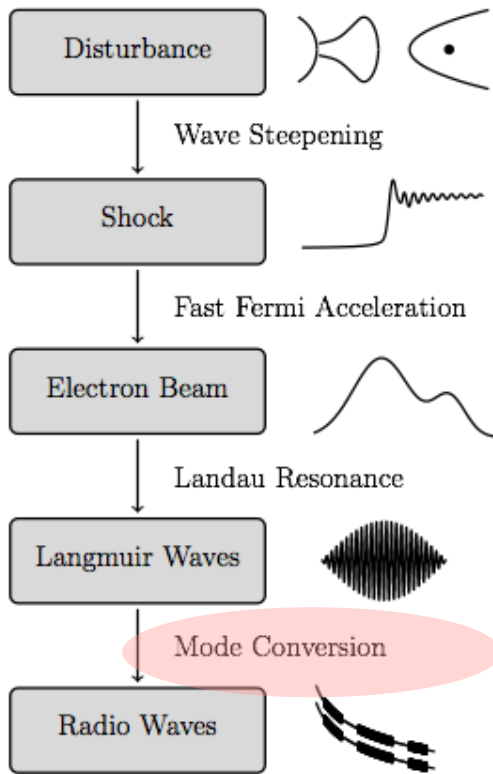
Summary of electromagnetic electron waves

conditions	dispersion relation	name
$\vec{B}_0 = 0$	$\omega^2 = \omega_p^2 + k^2 c^2$	light wave
$\vec{k} \perp \vec{B}_0, \vec{E}_1 \parallel \vec{B}_0$	$\frac{c^2 k^2}{\omega^2} = 1 - \frac{\omega_p^2}{\omega^2}$	O wave
$\vec{k} \perp \vec{B}_0, \vec{E}_1 \perp \vec{B}_0$	$\frac{c^2 k^2}{\omega^2} = 1 - \frac{\omega_p^2}{\omega^2} \frac{\omega^2 - \omega_p^2}{\omega^2 - \omega_h^2}$	X wave
$\vec{k} \parallel \vec{B}_0$ (right circ. pol.)	$\frac{c^2 k^2}{\omega^2} = 1 - \frac{\omega_p^2/\omega^2}{1 - (\omega_c/\omega)}$	R wave (whistler mode)
$\vec{k} \parallel \vec{B}_0$ (left circ. pol.)	$\frac{c^2 k^2}{\omega^2} = 1 - \frac{\omega_p^2/\omega^2}{1 + (\omega_c/\omega)}$	L wave

We also need Langmuir waves and ion sound waves

$$\omega^2 = \omega_{pe}^2 + 3/2 k^2 v_{th}^2 \quad \text{and} \quad \omega = k c_s$$

Physics - Plasma Radio Emission



- Mostly understood and measured
- One outstanding issue is mode conversion
 - nonlinear RPA wave-coupling
 - linear mode-coupling in density gradients

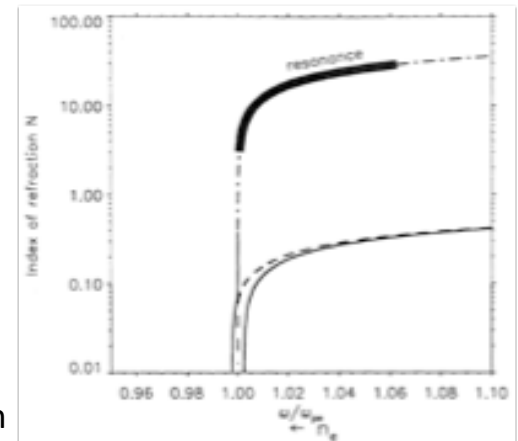
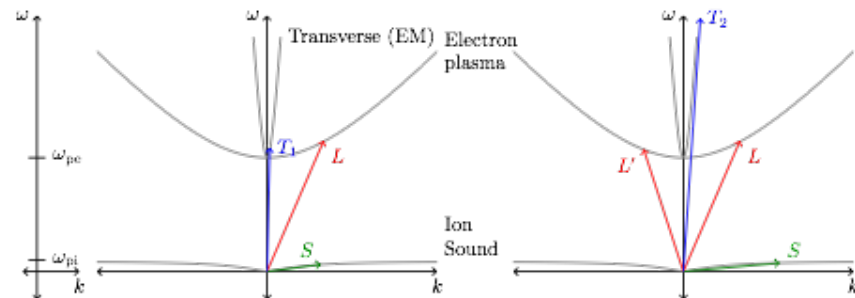


Figure 11. The dispersion relation of electron plasma waves, as index of refraction ($N = kc/\omega$) against ω/ω_{pe} . The dot-dash line is the warm plasma, magnetized Langmuir mode, which meets the electromagnetic α -mode at small N . Waves with beam speeds discussed in this paper have a resonant refractive index marked by the heavy bar. As they propagate into density enhancements, they must move leftward on the curve, and hence down to very small wavenumber.

Strong scattering!



Electrostatic Decay: Theory

- Langmuir waves generated by electron beams at Landau resonance $k_b = \frac{\omega_p}{v_b}$

- Langmuir waves can decay into backward propagating Langmuir waves: $L \rightarrow L' + S$.

- By assuming the linear dispersion relations

$$\omega_L = \omega_p + \frac{3v_e^2 k^2}{2\omega_p} \quad \text{and} \quad \omega_S = v_s k \quad \text{the wave numbers are:}$$

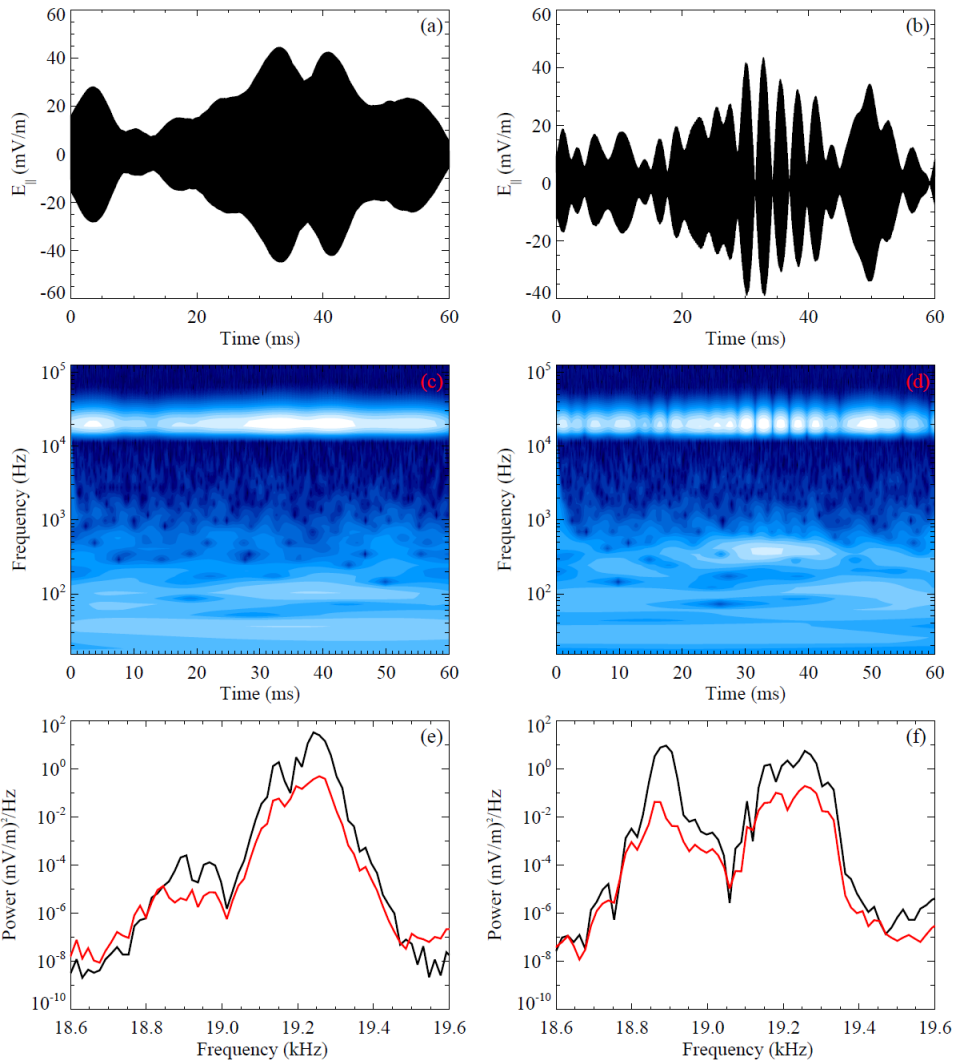
$$k_L = k_b,$$

$$k_{L'} = -k_b + k_0,$$

$$k_S = 2k_b - k_0,$$

$$\text{where } k_0 = 2\omega_p v_s / 3v_e^2$$

Evidence of electrostatic decay



- STEREO events on 2011 January 22.
- Panels: waveforms of E_{par} , wavelet transforms, and power spectra.
- Left: before ES decay.
- Right: during ES decay.
- Observed and expected frequency differences agree ($360 \pm 80 \text{ Hz}$ versus $300 \pm 90 \text{ Hz}$).

Langmuir eigenmodes in density cavities (Ergun et al.)

Eigenmode Solutions for Langmuir Electric field

$$E(x, t) = \sum_n^{\infty} A_n E_n$$

Envelope

Plasma Oscillation

$$E_n = H_n(Qx) e^{-\frac{(Qx)^2}{2}} e^{i(k+\Delta k)x - i(\omega+\Delta\omega)t + \phi}$$

$$Q^2 = \frac{\omega_{plasma}}{\sqrt{3}v_e L}$$

$$v_e = \sqrt{\frac{k_b T_e}{m_e}}$$

$$\Delta k = -\frac{\omega_{plasma} v_{\Delta}}{3v_e^2}$$

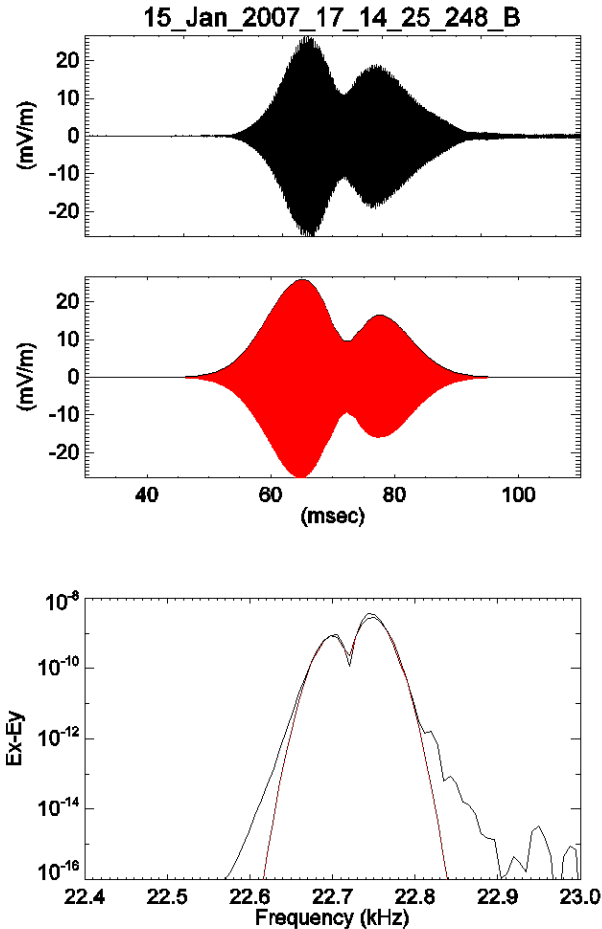
$$v_{\Delta} = v_{group} - v_{sound}$$

$$\Delta\omega = \frac{(2n+1)\sqrt{(3)}v_e}{2L} - \frac{v_{\Delta}^2 \omega_{plasma}}{6v_e^2}$$

Quantization condition

Langmuir eigenmodes in density cavities (Ergun et al.)

Case Study Fits (More Complex)

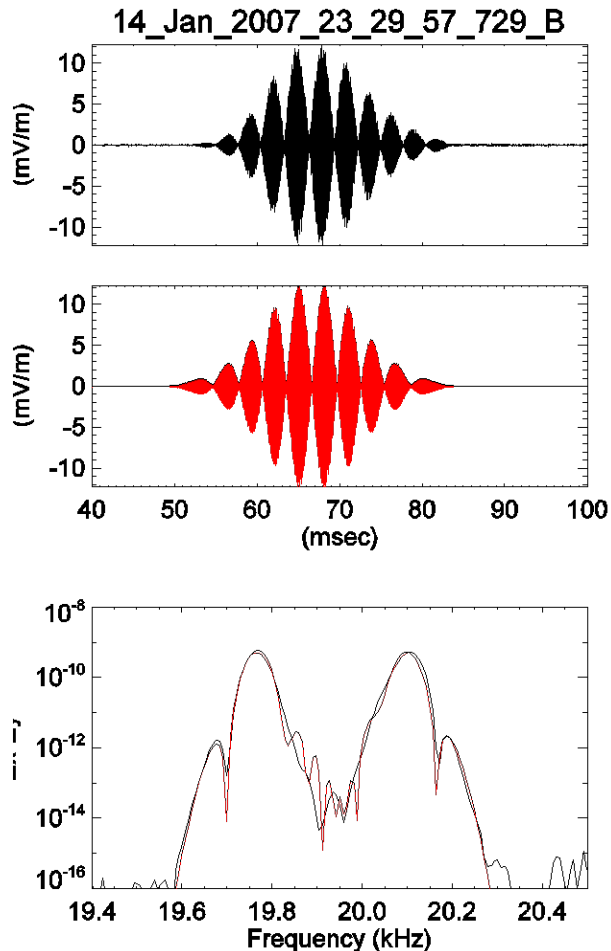


<u>mode</u>	<u>An</u>
0	0.45
1	0.5
2	0.05

<u>Param.</u>	<u>Val.</u>	<u>Unit</u>
Vb	0.24*c	m/s
Vsw * B/ B	600	km/s
Q	0.0002	1/m
Te	4.9e5	K
fp	22.8	kHz
Length	15.8	km
Vg	311	km/s
Ve	2733	km/s
W	5e-5	
k/Q	7.43	

Langmuir eigenmodes in density cavities (Ergun et al.)

Case Study Fits (Very Complex)



mode	<u>An</u>
1	-0.06
2	-0.0006
3	-0.222
5	0.35
7	-0.26
8	-0.0013
9	-0.0059
11	0.097

<u>Param.</u>	<u>Val.</u>	<u>Unit</u>
Vb	0.2*c	m/s
Vsw * B/ B	280	km/s
Q	0.0012	1/m
Te	7091 *(2-4)	K
fp	20.2	kHz
Length	3.31	km
Vg	6	km/s
Ve	328	km/s
W	1e-3	
k/Q	4.99	

Linear mode conversion

- Langmuir waves generated at Landau resonance
- Scattering in solar wind density fluctuation
- WKB propagation – conservation of energy flux
- Langmuir \rightarrow z-mode (e/m)
- Z-mode tunnels into o-mode (for small ω_c/ω_p)

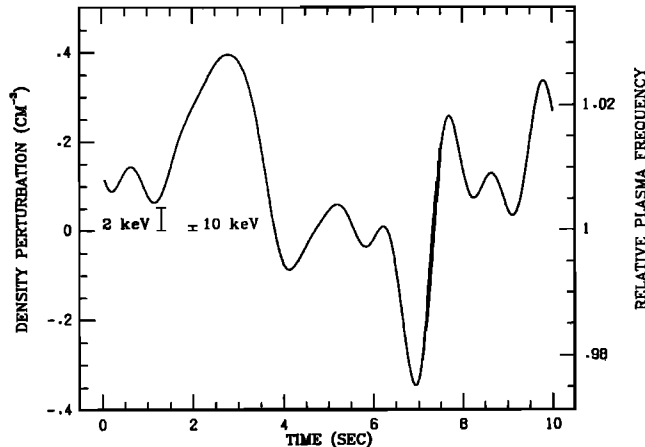


Figure 1. A time series of density fluctuations reconstructed from an averaged spectrum [Neugebauer, 1976]. The two brackets at the left show the difference between the plasma frequency and the resonant frequency for electron beams of 2 and 10 keV.

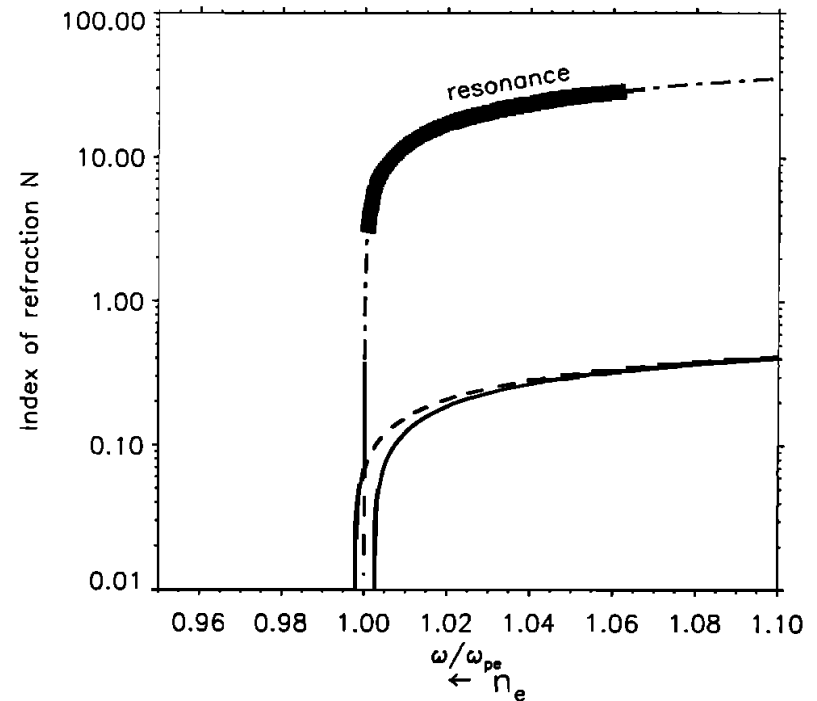
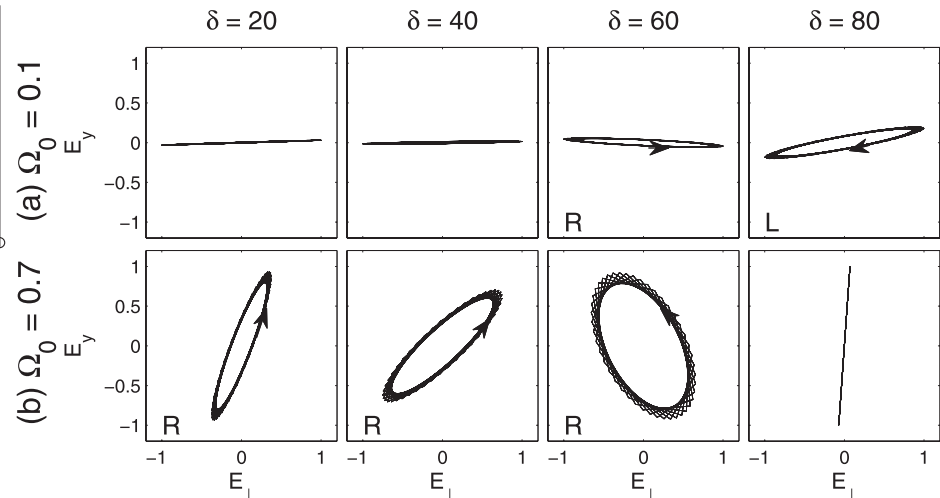
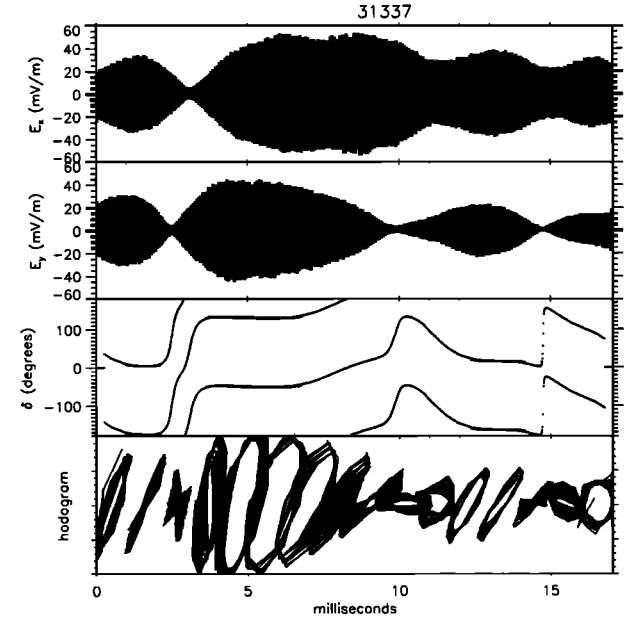
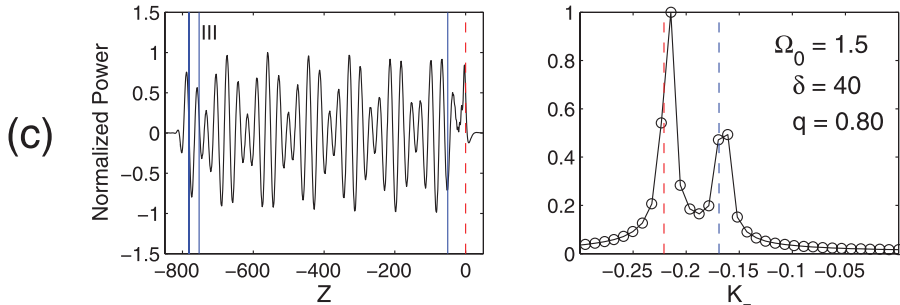
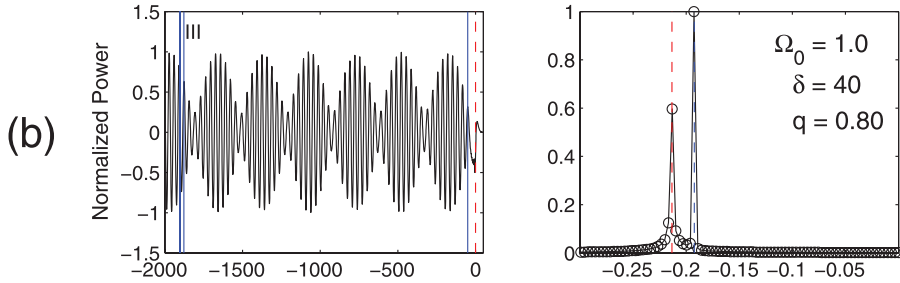
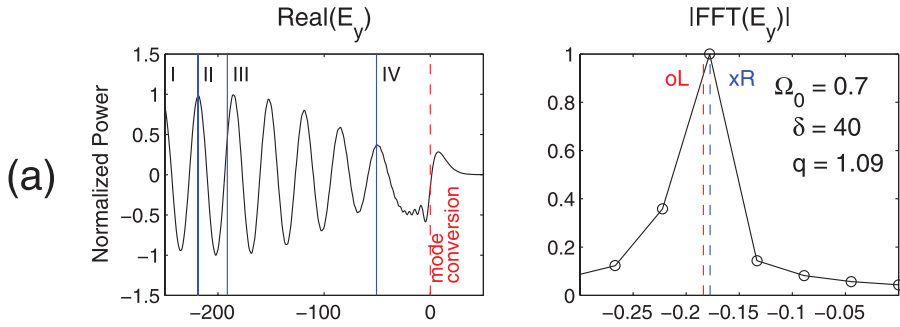


Figure 11. The dispersion relation of electron plasma waves, as index of refraction ($N = kc/\omega$) against ω/ω_{pe} . The dot-dash line is the warm plasma, magnetized Langmuir mode, which meets the electromagnetic z-mode at small N . Waves with beam speeds discussed in this paper have a resonant refractive index marked by the heavy bar. As they propagate into density enhancements, they must move leftward on the curve, and hence down to very small wavenumber.

Linear mode conversion: evidence

122103-5 Kim, Cairns, and Johnson



It's linear!
polarization signatures

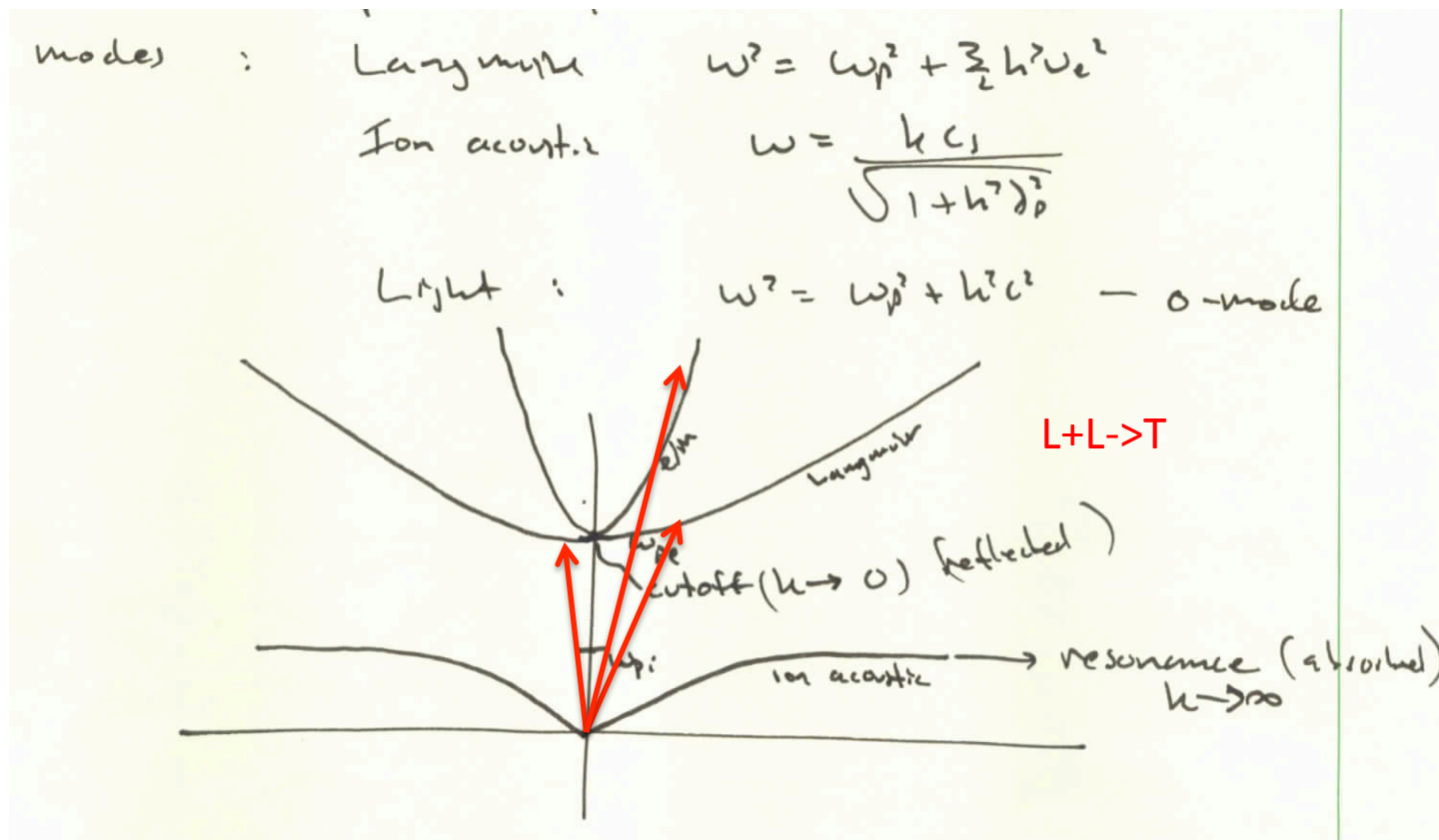
Three-wave RPA processes

$$\omega_{L1} + \omega_{L2} = \omega_T$$

L+L->T ($2f_{pe}$)

L+S->T (f_{pe})

$$k_{L1} + k_{L2} = k_T \ll k_L$$



Some outstanding issues

- Type III electron beam generation: flare physics, reconnection
- Type III beam regeneration and propagation (Sturrock, Kontar)
- Mode conversion problem: linear vs nonlinear (including 4 wave)
- Are Langmuir eigenmodes important?
- Fundamental vs harmonic emission in type II and III
- Is foreshock structure important to type II emission?